THE JOURNAL OF PHYSICAL CHEMISTRY B

ARTICLE

pubs.acs.org/JPCB

Electroosmotic Velocity and Electric Conductivity in a Fibrous Porous Medium in the Transverse Direction

Huan J. Keh* and Yi Y. Wu

Department of Chemical Engineering, National Taiwan University, Taipei 10617, Taiwan, Republic of China

ABSTRACT: The steady electroosmosis and electric conduction in a fibrous medium constructed by a homogeneous array of parallel, identical, charged, circular cylinders filled with an electrolyte solution is analytically examined. The imposed electric field is constant and normal to the axes of the cylinders. The electric double layer surrounding each dielectric cylinder may have an arbitrary thickness relative to the radius of the cylinder. A unit cell model that allows for the overlap of the double layers of adjacent cylinders is employed. The electrokinetic equations that govern the ionic concentration distributions, the electrostatic potential profile, and the fluid flow field in the electrolyte solution surrounding the charged cylinder in a cylindrical cell are linearized assuming that the system is only slightly distorted from equilibrium. Through the use of a regular perturbation method, these linearized equations are solved with the surface charge density (or zeta potential) of the cylinder as the small perturbation parameter. Analytical expressions for the electroosmotic velocity of the fluid solution and the effective electric conductivity in the array of cylinders are obtained in closed forms as functions of the porosity of the fiber matrix and other characteristics of the porous system. Comparisons of the results of the cell model with different conditions at the outer boundary of the cell are made. The cell model predicts that, under otherwise identical conditions, the electric conductivity in a porous medium composed of an array of parallel cylinders in the transverse direction in general is smaller than that of a suspension of spheres, but there are some exceptions. The effect of interactions among the cylinders or spheres on the effective conductivity can be significant under appropriate conditions.

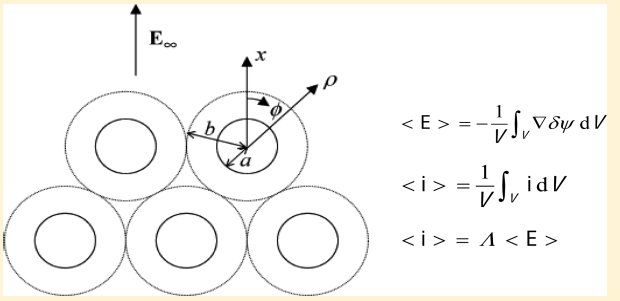

1. INTRODUCTION

When a charged solid surface is in contact with an electrolyte solution, it is surrounded by a diffuse cloud of ions carrying a total charge equal and opposite in sign to that of the solid surface. This distribution of fixed charge and adjacent diffuse ions is known as an electric double layer. For a suspension of charged particles or a charged porous medium subject to an external electric field, the solid entities and/or the surrounding mobile ions are driven to migrate. As a result, the fluid solution is dragged to flow by the motions of the solid entities and/or the ions, and there exists an electric current through the suspension or porous medium. In practical applications, it is necessary to determine not only the electrophoretic or electroosmotic velocity, but also the average current density and effective electric conductivity in the suspension or porous system.

Assuming that the electric double layer is not distorted from the equilibrium state, Henry[1] derived analytical expressions for the electrophoretic mobility of a dielectric sphere and of a long cylinder of radius a with small zeta potential ζ for the entire range of κa, where κ is the reciprocal Debye screening length (defined right after eq 10). Booth[2] extended Henry's analysis to include the effect of ionic convection in the diffuse layer and determined the electrophoretic mobility of a charged sphere as a power series in ζ. On the other hand, Dukhin and Derjaguin[3] derived a simple formula for the effective electric conductivity of a dilute suspension of charged spheres considering an infinite plane slab of suspension immersed in an infinite homogeneous electrolyte subject to an electric field perpendicular to the plane slab. Extending this analysis, Saville[4] and O'Brien[5] assumed that the particles and their double layers occupy only a small fraction of the total volume of the suspension to obtain approximate formulas for the electric conductivity using a perturbation method for particles with low zeta potential immersed in a symmetrically charged electrolyte correct to $O(\zeta^2)$.

Later, approximate analytical expressions for the electrophoretic mobility and electric conductivity of a dilute suspension of colloidal spheres with an arbitrary zeta potential and thin double layers in symmetric electrolytes correct to order $(\kappa a)^{-1}$ were obtained by Ohshima et al.[6] When the zeta potential of the particles is small, their results are in agreement with Henry's[1] and O'Brien's.[5] O'Brien[7] also derived analytical formulas for the electrophoretic mobility and electric conductivity of a dilute suspension of dielectric spheres with thin but polarized double layers in a general electrolyte solution. The agreement between these formulas and the general numerical solutions[8] is good for all reasonable values of the zeta potential when $\kappa a > 20$. Using a

Received: April 26, 2011
Revised: June 10, 2011
Published: June 14, 2011

dx.doi.org/10.1021/jp203890n | J. Phys. Chem. B 2011, 115, 9168–9178

similar analysis, O'Brien and Ward[9] also determined the electrophoretic mobility and electric conductivity of a dilute suspension of randomly oriented spheroids with thin polarized diffuse layers at the particle surfaces.

In practical applications of the electrophoresis/electroosmosis and electric conduction, relatively concentrated suspensions of particles or porous media with a relatively low porosity are usually encountered, and the effect of interactions among the solid entities will be important. To avoid the difficulty of the complex geometry appearing in assemblages of solid entities, the unit cell model was used by many researchers to predict the effect of entity interactions on various transport properties such as the mean sedimentation rate,[10−18] the average electrophoretic/electroosmotic velocity,[19−33] effective electric conductivity,[28−37] and diffusiophoretic/diffusioosmotic velocity[38−41] in bounded suspensions or porous systems of identical solid entities. This model involves the concept that an assemblage can be divided into a number of identical cells, one solid entity occupying each cell at its center. The boundary-value problem for multiple entities is thus reduced to the consideration of the behavior of a single entity and its bounding envelope. Although different shapes of the cell can be employed, the assumption of a spherical[12−19,26−34,39−41] or cylindrical[11,20,22,25,35,38] shape for the fictitious envelope of fluid solution surrounding each spherical or cylindrical entity is of great convenience.

The electrophoresis/electroosmosis and electric conduction in a concentrated suspension or porous system of identical dielectric spheres with a small surface potential and an arbitrary double-layer thickness were analyzed using the unit cell model.[30] Closed-form formulas for the electrophoretic/electroosmotic velocity and electric conductivity were obtained as functions of κa and the volume fraction of the particles correct to $O(\zeta^2)$. It was found that these formulas agree relatively well with the available experimental data for suspensions of spherical particles with various volume fractions[42,43] in comparison with the predictions obtained earlier by Anderson,[44] O'Brien,[5] and Ohshima.[34]

In the present work, the previous cell-model analysis for the electrophoretic/electroosmotic velocity and electric conductivity in a monodisperse suspension of charged spheres with an arbitrary thickness of the electric double layers[30] is extended to a fibrous medium constructed by a homogeneous array of parallel charged circular cylinders. The overlap of adjacent double layers is allowed, and the relaxation effect in the diffuse layer surrounding each cylinder is taken into account appropriately. The analytical solutions in closed forms obtained with the cylindrical cell model enable the electroosmotic velocity and electric conductivity to be predicted as functions of the porosity of the fiber matrix and other characteristics of the system for various cases. Comparisons of the results between a system of parallel cylinders and a system of spheres will be given.

2. ELECTROKINETIC EQUATIONS

We consider a liquid solution containing M ionic species filled in a fibrous porous medium constructed by a uniform array of parallel, identical, charged, circular cylinders. When the system is subjected to a constant applied electric field $E_\infty \mathbf{e}_x$, the solution moves with a bulk (superficial) velocity equal to $-U\mathbf{e}_x$ relative to the array at the steady state due to electroosmosis/electrophoresis, where $\mathbf{e}_x$ is the unit vector in the positive x direction, which is perpendicular to the axes of the cylinders. The ions can diffuse freely in the fibrous porous medium, so there exists no regular osmotic flow of the solvent. As shown in Figure 1, we employ a unit cell model in which each dielectric cylinder of radius a is surrounded by a coaxial circular

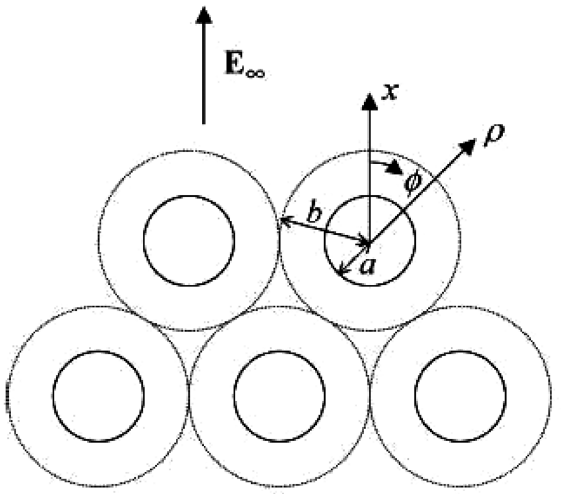

Figure 1. Geometrical sketch of the unit cell model for a homogeneous array of parallel, identical, circular cylinders.

cylindrical shell of the fluid solution having an outer radius of b such that the fluid/cell volume ratio is equal to the porosity $1 - \varphi$ of the fiber matrix, viz., $\varphi = (a/b)^2$. The cell as a whole is electrically neutral. The origin of the polar coordinate system (ρ,φ) is taken at the axis of the cylinder, and the polar axis $\varphi = 0$ points toward the positive x direction. Obviously, the two-dimensional problem for each cell is symmetric about the x-axis.

2.1. Governing Equations. It is assumed that the magnitude of the fluid velocity relative to the cylinder is not large and hence that the electric double layer surrounding the cylinder is only slightly distorted from the equilibrium state, where there is no applied electric field and the fluid is at rest. Therefore, the concentration (number density) distribution $n_m(\rho,\varphi)$ of the species m, the electrostatic potential distribution $\psi(\rho,\varphi)$, and the dynamic pressure distribution $p(\rho,\varphi)$ can be expressed as

$$n_m = n_m^{(\mathrm{eq})} + \delta n_m \tag{1a}$$

$$\psi = \psi^{(\mathrm{eq})} + \delta\psi \tag{1b}$$

$$p = p^{(\mathrm{eq})} + \delta p \tag{1c}$$

where $n_m^{(\mathrm{eq})}(\rho)$, $\psi^{(\mathrm{eq})}(\rho)$, and $p^{(\mathrm{eq})}(\rho)$ are the equilibrium distributions of the concentration of the species m, electrostatic potential, and dynamic pressure, respectively, and $\delta n_m(\rho,\varphi)$, $\delta\psi(\rho,\varphi)$, and $\delta p(\rho,\varphi)$ are the small perturbations to the equilibrium state. The equilibrium concentration of each ionic species is related to the equilibrium potential by the Boltzmann distribution. The local electric field $\mathbf{E}(\rho,\varphi) = -\nabla\psi$.

It can be shown that the small perturbed quantities δn_m, $\delta\psi$, and δp together with the fluid velocity field $\mathbf{u}(\rho,\varphi)$ satisfy the following set of linearized electrokinetic equations:[30]

$$\eta\nabla^2\mathbf{u} = \nabla\delta p - \varepsilon[\nabla^2\psi^{(\mathrm{eq})}\nabla\delta\psi + \nabla^2\delta\psi\nabla\psi^{(\mathrm{eq})}] \tag{2}$$

$$\nabla\cdot\mathbf{u} = 0 \tag{3}$$

$$\nabla^2\delta\mu_m = \frac{z_m e}{kT}\left[\nabla\psi^{(\mathrm{eq})}\cdot\nabla\delta\mu_m - \frac{kT}{D_m}\nabla\psi^{(\mathrm{eq})}\cdot\mathbf{u}\right], \quad m = 1,2,\ldots,M \tag{4}$$

dx.doi.org/10.1021/jp203890n |J. Phys. Chem. B 2011, 115, 9168–9178

Here, $\delta\mu_m$ is defined as a linear combination of δn_m and $\delta\psi$ on the basis of the concept of the electrochemical potential energy,[6]

$$\delta\mu_m = \frac{kT}{n_m^{(eq)}}\delta n_m + z_m e\delta\psi \quad (5)$$

η and ε are the viscosity and dielectric permittivity, respectively, of the fluid; D_m and z_m are the diffusion coefficient and valence, respectively, of the species m; e is the elementary electric charge; k is Boltzmann's constant; T is the absolute temperature. In eqs 2 and 4, D_m, η, and ε are assumed to be constant in the fluid phase.

2.2. Boundary Conditions. The boundary conditions for $\mathbf{u}$ and $\delta\mu_m$ at the surface of the dielectric cylinder are

$$\rho = a: \quad \mathbf{u} = 0 \quad (6a)$$

$$\frac{\partial\delta\mu_m}{\partial\rho} = 0 \quad (6b)$$

which are obtained from the assumptions that the "shear plane" coincides with the cylinder surface, the Gauss condition holds at the surface, and no ions can penetrate into the cylinder. The effect of conductance behind the shear plane is neglected.

At the outer (virtual) surface of the cell, the local electric field should be compatible with the uniform applied field $E_\infty\mathbf{e}_x$, according to the Levine–Neale electrokinetic model.[19,22,25] Thus, the boundary conditions over there are

$$\rho = b: \quad u_\rho = -U\cos\phi \quad (7a)$$

$$\tau_{\rho\phi} = \eta\left[\rho\frac{\partial}{\partial\rho}\left(\frac{u_\phi}{\rho}\right) + \frac{1}{\rho}\frac{\partial u_\rho}{\partial\phi}\right] = 0 \quad \text{(for the Happel model)} \quad (7b)$$

$$(\nabla\times\mathbf{u})_z = \frac{1}{\rho}\frac{\partial}{\partial\rho}(\rho u_\phi) - \frac{1}{\rho}\frac{\partial u_\rho}{\partial\phi} = 0 \quad \text{(for the Kuwabara model)} \quad (7c)$$

$$\frac{\partial\delta\mu_m}{\partial\rho} = -z_m eE_\infty\cos\phi \quad (7d)$$

where U is the electroosmotic velocity to be determined, and u_ρ and u_φ are the ρ and φ components, respectively, of $\mathbf{u}$. The Happel hydrodynamic model[10,11] assumes that the radial velocity relative to the bulk flow and the shear stress of the fluid on the outer boundary of the cell are zero, whereas the Kuwabara hydrodynamic model[12] assumes that this radial velocity and the vorticity of the fluid are zero there.

For the sedimentation of a suspension of uncharged spherical particles, both the Happel and the Kuwabara models give qualitatively the same flow fields and approximately comparable drag forces on the particle in a cell. However, the Happel model has significant advantage in that it does not require an exchange of mechanical energy between the cell and the environment.[45]

The boundary condition of the electric potential at the virtual surface $\rho = b$ may alternatively be taken as the distribution giving rise to the applied electric field in the cell, known as the Zharkikh–Shilov electrokinetic model.[20,21,26] In this case, eq 7d becomes

$$\rho = b: \quad \delta\mu_m = -z_m eE_\infty\rho\cos\phi \quad (8)$$

Note that the overlap of the electric double layers of adjacent cylinders is allowed in both of the boundary conditions given by eqs 7d and 8.

3. SOLUTIONS FOR THE ELECTROOSMOTIC VELOCITY

3.1. Solution for the Equilibrium Electrostatic Potential. Before solving for the problem of electroosmosis around a charged cylinder in a unit cell filled with the solution of M ionic species, we need to determine the equilibrium electrostatic potential in the fluid phase first. The equilibrium potential $\psi^{(eq)}$ satisfies the Poisson–Boltzmann equation, the Gauss condition at the cylinder surface $\rho = a$, and the requirement of no electric current passing through the virtual surface $\rho = b$. It is easy to show that

$$\psi^{(eq)} = \psi_{eq1}(\rho)\bar{\sigma} + O(\bar{\sigma}^2) \quad (9)$$

where $\bar{\sigma} = e\sigma/\varepsilon\kappa kT$, which is the nondimensional quantity of the uniform surface charge density σ of the cylinder, and

$$\psi_{eq1}(\rho) = \frac{kT}{e}\frac{I_1(\kappa b)K_0(\kappa\rho) + I_0(\kappa\rho)K_1(\kappa b)}{I_1(\kappa b)K_1(\kappa a) - I_1(\kappa a)K_1(\kappa b)} \quad (10)$$

Here, I_n and K_n are the modified Bessel functions of order n of the first and second kinds, respectively, κ is the Debye screening parameter equal to $(e^2\Sigma_{m=1}^{M} z_m^2 n_m^\infty/\varepsilon kT)^{1/2}$, and n_m^∞ is the concentration of the type m ions in the bulk (electrically neutral) solution where the equilibrium potential is set equal to zero. Equation 9 for $\psi^{(eq)}$ as a power series in the surface charge density of the cylinder up to $O(\bar{\sigma})$ is the equilibrium solution to the linearized Poisson–Boltzmann equation that is valid for small values of the electric potential (the Debye–Huckel approximation). That is, the surface charge density must be sufficiently small for the potential field $\psi^{(eq)}$ to remain small. Note that the contribution from the $\bar{\sigma}^2$ term to $\psi^{(eq)}$ in eq 9 disappears for the case of symmetric electrolytes.

Using eqs 9 and 10, one obtains a relation between the surface potential and the surface charge density of the dielectric cylinder in a unit cell at equilibrium,

$$\bar{\sigma} = W\frac{e\zeta}{kT} \quad (11)$$

where

$$W = \frac{I_1(\kappa b)K_1(\kappa a) - I_1(\kappa a)K_1(\kappa b)}{I_1(\kappa b)K_0(\kappa a) + I_0(\kappa a)K_1(\kappa b)} \quad (12)$$

and $\zeta = \psi^{(eq)}(a)$, which is the equilibrium surface potential (known as the zeta potential) of the cylinder. Namely, the solution for $\psi^{(eq)}(\rho)$ given by eq 9 with the substitution of eq 11 is also valid for a dielectric cylinder with a constant surface potential in the cell.

3.2. Solution of the Electrokinetic Equations and Electroosmotic Velocity. To solve for the small quantities $\mathbf{u}$, δp, and $\delta\mu_m$ and the electroosmotic velocity U for the case of small parameter $\bar{\sigma}$, these variables are written as perturbation expansions in powers of $\bar{\sigma}$,

$$\mathbf{u} = \mathbf{u}_1\bar{\sigma} + \mathbf{u}_2\bar{\sigma}^2 + \cdots \quad (13a)$$

$$\delta p = p_1\bar{\sigma} + p_2\bar{\sigma}^2 + \cdots \quad (13b)$$

$$\delta\mu_m = z_m e\psi_0 + \mu_{m1}\bar{\sigma} + \mu_{m2}\bar{\sigma}^2 + \cdots \quad (13c)$$

$$U = U_1\bar{\sigma} + U_2\bar{\sigma}^2 + \cdots \quad (13d)$$

dx.doi.org/10.1021/jp203890n |J. Phys. Chem. B 2011, 115, 9168–9178

where the functions $\mathbf{u}_i$, p_i, μ_{mi}, and U_i are independent of $\bar{\sigma}$. It is easy to show that, in eq 13c,

$$\psi_0 = -E_\infty \frac{\rho}{\chi}\left[1+\left(\frac{a}{\rho}\right)^2\right] cos\ \phi \tag{14}$$

where the coefficient χ equals $1-\varphi$ when condition 7d for the Levine−Neale model is used, and equals $1+\varphi$ when condition 8 for the Zharkikh−Shilov model is used.

Substituting the expansions given by eqs 13 and $\psi^{(eq)}$ given by eq 9 into the governing eqs 2−4 and boundary conditions 6, 7a, either 7b or 7c, and either 7d or 8, and equating like powers of $\bar{\sigma}$ on both sides of the respective equations, one can derive a group of linear differential equations and boundary conditions for each set of the functions $\mathbf{u}_i$, p_i, and μ_{mi} with i equal to 1, 2, ... After collecting the first-order terms in the perturbation procedure, we obtain

$$\nabla^2\mathbf{u}_1 = \frac{1}{\eta}\nabla p_1 - \frac{\varepsilon}{\eta}\nabla^2\psi_{eq1}\nabla\psi_0 \tag{15a}$$

$$\nabla\cdot\mathbf{u}_1 = 0 \tag{15b}$$

$$\nabla^2\mu_{m1} = -\frac{z_m^2 e^2 E_\infty}{kT\chi}\left[1-\left(\frac{a}{\rho}\right)^2\right]\frac{d\psi_{eq1}}{d\rho} cos\ \phi \tag{16}$$

with

$$\rho = a: \quad \mathbf{u}_1 = 0 \tag{17a}$$

$$\frac{\partial\mu_{m1}}{\partial\rho} = 0 \tag{17b}$$

$$\rho = b: \quad u_{1\rho} = -U_1\ cos\ \phi \tag{18a}$$

$$\tau_{1\rho\phi} = 0 \quad \text{(for the Happel model)} \tag{18b}$$

$$(\nabla\times\mathbf{u}_1)_z = 0 \quad \text{(for the Kuwabara model)} \tag{18c}$$

$$\frac{\partial\mu_{m1}}{\partial\rho} = 0 \quad \text{(for the Levine−Neale model)} \tag{18d}$$

$$\mu_{m1} = 0 \quad \text{(for the Zharkikh−Shilov model)} \tag{18e}$$

The solutions for μ_{m1}, p_1, and the ρ and φ components of $\mathbf{u}_1$ subject to eqs 15−18 are

$$u_{1\rho} = E_\infty F_{1\rho}(\rho)\ cos\ \phi \tag{19a}$$

$$u_{1\phi} = E_\infty F_{1\phi}(\rho)\ sin\ \phi \tag{19b}$$

$$p_1 = E_\infty\left[\frac{\eta}{a}F_{p1}(\rho) - \frac{\varepsilon\kappa^2}{\chi}\left(\rho+\frac{a^2}{\rho}\right)\psi_{eq1}(\rho)\right] cos\ \phi \tag{19c}$$

$$\mu_{m1} = E_\infty F_{m1}(\rho)\ cos\ \phi \tag{20}$$

where the functions $F_{1\rho}(\rho)$, $F_{1\varphi}(\rho)$, $F_{p1}(\rho)$, and $F_{m1}(\rho)$ are defined by eqs A1 and A2 in the Appendix.

Since the unit cell as a whole is electrically neutral, the net force exerted on its virtual surface must be zero. Applying this constraint to eqs 19 and A1, we obtain the first-order term for the electroosmotic velocity of the fluid expressed as

$$U_1 = -\frac{\varepsilon E_\infty(\kappa a)^2}{8\eta(1+\varphi^2)\chi}\left\{\frac{(1+\varphi)\psi_{eq1}(b)}{\varphi\omega} + \int_a^b\left(1+\frac{a^2}{\rho^2}\right)\left[1-\frac{\rho^2}{a^2}\left(1-2\ ln\frac{\rho}{a}\right) + \varphi^2\frac{\rho^2}{a^2}\left(1+2\ ln\frac{\rho}{a}-\frac{\rho^2}{a^2}\right)\right]\frac{d\psi_{eq1}}{d\rho}d\rho\right\} \tag{21a}$$

for the Happel model, and

$$U_1 = -\frac{\varepsilon E_\infty(\kappa a)^2}{8\eta\chi}\left\{\frac{3(1+\varphi)\psi_{eq1}(b)}{2\varphi\omega'} + \int_a^b\left(1+\frac{a^2}{\rho^2}\right)\left[1-\frac{\rho^2}{a^2}\left(1-2\ ln\frac{\rho}{a}\right) - \frac{1}{2}\varphi\left(1-2\frac{\rho^2}{a^2}+\frac{\rho^4}{a^4}\right)\right]\frac{d\psi_{eq1}}{d\rho}d\rho\right\} \tag{21b}$$

for the Kuwabara model. In eqs 21, the function $\psi_{eq1}(\rho)$ is given by eq 10 and ω and ω' are functions of φ defined by eqs A9. Taking $\chi = 1-\varphi$ (viz., using the Levine−Neale model for the electric potential at the virtual surface of the cell), one can find that eq 21b is identical to the result obtained by Kozak and Davis[22] for the electroosmotic velocity of the fluid in an ordered array of parallel charged cylinders.

Substitution of eq 11 into eq 13d results in an expression for the electroosmotic velocity of the solution as a perturbation expansion in powers of ζ,

$$U = \frac{e}{kT}WU_1\zeta + O(\zeta^2) \tag{22}$$

Note that, for the case of a symmetric electrolyte, U_2, the contribution from the term of σ^2 or ζ^2 to U, disappears. Also, the relaxation effect of the diffuse ions in the electric double layer surrounding the cylinder is not included in eq 22 up to the order ζ.

Among the second-order terms in the perturbation procedure, the only distributions we need in the following calculations for the electric conductivity are the electrochemical potential energies μ_{m2}. If the solution contains only a symmetrically charged electrolyte ($M = 2$, $z_+ = -z_- = Z$, $n_+^\infty = n_-^\infty = n^\infty$, where the subscripts + and − refer to the cation and anion, respectively), the equation governing $\mu_{\pm2}$ is

$$\nabla^2\mu_{\pm2} = \pm\frac{Ze}{kT}\nabla\psi_{eq1}\cdot\left(\nabla\mu_{\pm1} - \frac{kT}{D_\pm}\mathbf{u}_1\right) \tag{23}$$

The boundary conditions for $\mu_{\pm2}$ are given by eqs 17b and either 18d or 18e with the subscript 1 replaced by 2. The solution for $\mu_{\pm2}$ is obtained as

$$\mu_{\pm2} = E_\infty F_{\pm2}(\rho)\ cos\ \phi \tag{24}$$

where the functions $F_{\pm2}(\rho)$ are defined by eq A10. For a general electrolyte, there is an extra term on the right-hand side of eq 23 involving the $O(\bar{\sigma}^2)$ correction to the equilibrium potential as expressed by eq 9. This extra term considerably complicates the problem. So we consider here only the case of a symmetric electrolyte, in which the $O(\bar{\sigma}^2)$ term in eq 9 vanishes and the leading correction to $\psi_{eq\ 1}\bar{\sigma}$ is $O(\bar{\sigma}^3)$.

dx.doi.org/10.1021/jp203890n |J. Phys. Chem. B 2011, 115, 9168–9178

4. SOLUTION FOR THE ELECTRIC CONDUCTIVITY

4.1. Formulation for the Electric Conductivity. When the ordered array of parallel charged cylinders is subjected to a constant external electric field $\mathbf{E}_\infty$ normal to the cylinder axes, the effective electric conductivity in this fibrous medium can be determined from the solution for the fluid velocity and electrochemical potential energies obtained in the previous section. The average of the local electric field can be expressed as

$$\langle \mathbf{E} \rangle = -\frac{1}{V}\int_V \nabla \delta\psi \, dV \tag{25}$$

where V denotes a sufficiently large cylindrical volume of the fiber matrix to contain many cylinders. To obtain eq 25, we used eq 1b and the fact that the volume average of the gradient of the equilibrium electric potential is zero. There is a resulting volume-average current density, which is collinear with $\langle \mathbf{E} \rangle$, defined by

$$\langle \mathbf{i} \rangle = \frac{1}{V}\int_V \mathbf{i} dV \tag{26}$$

where $\mathbf{i}(\rho,\varphi)$ is the current density distribution. The effective electric conductivity Λ in the transverse direction of the fibrous medium can be assigned by the linear relation

$$\langle \mathbf{i} \rangle = \Lambda \langle \mathbf{E} \rangle \tag{27}$$

Since the measured electric field and current density are equal to $\langle \mathbf{E} \rangle$ and $\langle \mathbf{i} \rangle$, respectively, eq 27 is the usual experimental definition of electric conductivity, provided that the array of cylinders is everywhere homogeneous.

On the basis of the mathematical analysis given in a previous article,[30] the average current density is obtained as

$$\begin{aligned}\langle \mathbf{i} \rangle = \Lambda^\infty \langle \mathbf{E} \rangle + \frac{e}{\pi b k T}\sum_{m=1}^{M} z_m n_m^\infty D_m \int_0^{2\pi} \Bigg\{ z_m e\left(\psi_0 - \rho\frac{\partial \psi_0}{\partial \rho}\right) \\ + \overline{\sigma}\left[\rho\left(\frac{z_m^2 e^2}{kT}\psi_{eq1}\frac{\partial \psi_0}{\partial \rho} - \frac{\partial \mu_{m1}}{\partial \rho}\right) + \mu_{m1}\right] \\ + \overline{\sigma}^2\left[\rho\left(\frac{z_m e}{kT}\psi_{eq1}\frac{\partial \mu_{m1}}{\partial \rho} - \frac{z_m e}{D_m}\psi_{eq1} u_{1\rho} - \frac{\partial \mu_{m2}}{\partial \rho}\right.\right. \\ \left.\left. - \frac{z_m^3 e^3}{2k^2T^2}\psi_{eq1}^2\frac{\partial \psi_0}{\partial \rho}\right) + \mu_{m2} - \frac{z_m e}{kT}\psi_{eq1}\mu_{m1}\right] + O(\overline{\sigma}^3)\Bigg\}_{\rho=b} \mathbf{e}_\rho d\phi\end{aligned} \tag{28}$$

where $\Lambda^\infty = \sum_{m=1}^{M} z_m^2 e^2 n_m^\infty D_m/kT$, which is the electric conductivity of the electrolyte solution containing M ionic species in the absence of the cylinders, and $\mathbf{e}_\rho$ is the unit normal outward from the surface of the cylinder in a unit cell.

4.2. Solution for the Electric Conductivity. Substituting eqs 14, 19a, 20, and 24 into eq 28, making relevant calculations, and using the relations given by eqs 27 and 11, we obtain the electric conductivity in the array of parallel charged cylinders as a power series in ζ,

$$\begin{aligned}\Lambda = \Lambda^\infty\Bigg\{H + H^2 I\beta\frac{\zeta e}{kT} \\ + H^2\left[J_1\frac{\varepsilon k^2 T^2}{\eta(D_+ + D_-)e^2} + J_2 Z^2 + HI^2\beta^2\right]\left(\frac{\zeta e}{kT}\right)^2 + O(\zeta^3)\Bigg\}\end{aligned} \tag{29a}$$

for the Levine−Neale model, and

$$\Lambda = \Lambda^\infty\left\{H + I\beta\frac{\zeta e}{kT} + \left[J_1\frac{\varepsilon k^2 T^2}{\eta(D_+ + D_-)e^2} + J_2 Z^2\right]\left(\frac{\zeta e}{kT}\right)^2 + O(\zeta^3)\right\} \tag{29b}$$

for the Zharkikh−Shilov model. In these expressions,

$$\beta = \sum_{m=1}^{M} z_m^3 D_m n_m^\infty \Big/ \sum_{m=1}^{M} z_m^2 D_m n_m^\infty \tag{30}$$

$$H = \frac{1-\varphi}{1+\varphi} \tag{31}$$

$$I = -W\frac{e}{kT}\left[\frac{1-\varphi}{\chi}\psi_{eq1}(b) + \frac{\varphi}{\chi^2}\int_a^b \left(\frac{a^2}{\rho^2} - \frac{\rho^2}{a^2}\right)\frac{d\psi_{eq1}}{d\rho} d\rho\right] \tag{32}$$

for a general electrolyte, and

$$J_1 = W^2\frac{2\eta e^2}{\varepsilon k^2 T^2}\left[\frac{U_1}{E_\infty}\psi_{eq1}(b) + \frac{\varphi}{\chi}\int_a^b \left(1 + \frac{\rho^2}{a^2}\right)F_{1\rho}\frac{d\psi_{eq1}}{d\rho} d\rho\right] \tag{33a}$$

$$\begin{aligned}J_2 = W^2\frac{e^2}{2k^2T^2\chi}\Bigg[(1-\varphi)\psi_{eq1}^2(b) - \frac{2kT\varphi}{Z^2e^2}\int_a^b \left(1 + \frac{\rho^2}{a^2}\right)\frac{d\psi_{eq1}}{d\rho}\frac{dF_{\pm 1}}{d\rho} d\rho \\ + \frac{2\varphi}{\chi}\psi_{eq1}(b)\int_a^b \left(\frac{a^2}{\rho^2} - \frac{\rho^2}{a^2}\right)\frac{d\psi_{eq1}}{d\rho} d\rho\Bigg]\end{aligned} \tag{33b}$$

for a symmetrically charged electrolyte. In eqs 32 and 33, the function $\psi_{eq1}(\rho)$ is defined by eq 10. Note that the coefficients H, I, and J_2 are independent of the boundary condition for the fluid velocity prescribed at the virtual surface of the unit cell. In eqs 29, the relaxation effect in the electric double layer surrounding each cylinder caused by the convection of the fluid appears only through the coefficient J_1 of the $O(\zeta^2)$ term, whereas this polarization effect generated from the applied electric field directly is contained in the coefficients I and J_2. The numerical results of these coefficients and the normalized electric conductivity Λ/Λ^∞ calculated from eqs 29−33 as functions of the parameters κa and φ will be discussed in the next section.

5. RESULTS AND DISCUSSION

5.1. Electroosmotic Velocity. In Figures 2 and 3, the numerical values for the normalized electroosmotic velocity $U^* = \eta U/\varepsilon\zeta E_\infty$ of the fluid solution in the fibrous medium calculated from eq 22 incorporated with eqs 12 and 21 are plotted versus the parameters κa and φ for the unit cell model with various boundary conditions at the virtual surface of the cell. The calculations are presented up to $\varphi = 0.9$, which corresponds to the maximum attainable volume fraction (or minimum porosity) for a swarm of identical parallel cylinders (triangularly ordered).[46] It can be seen that this dimensionless electroosmotic velocity decreases monotonically with a decrease in κa (or with an increase in the double-layer overlap) for a specified value of φ. When $\kappa a = 0$, $U^* = 1/2$ as $\varphi = 0$, and $U^* = 0$ for all finite values of φ. The effect of the porosity $(= 1 - \varphi)$ of the fiber matrix on U^* can be significant even when the porosity is fairly high.

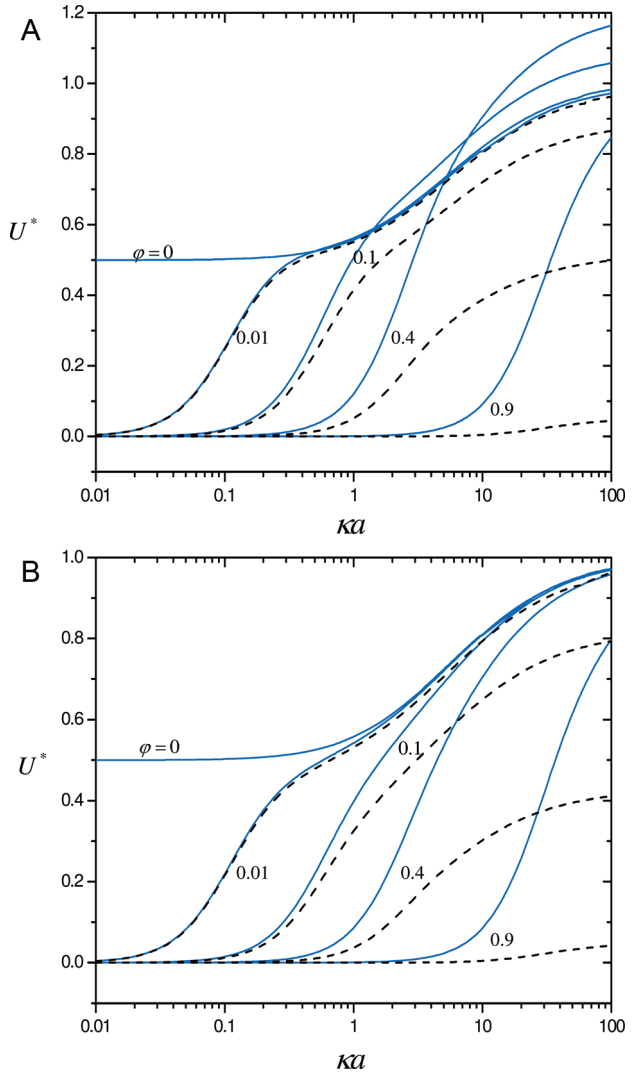

Figure 2. Plots of the normalized electroosmotic velocity U^* of an electrolyte solution through a transversely oriented fiber matrix versus κa with φ as a parameter: (a) the Happel hydrodynamic cell model; (b) the Kuwabara hydrodynamic cell model. The solid and dashed curves represent the predictions for the Levine−Neale and Zharkikh−Shilov electrokinetic cell models, respectively.

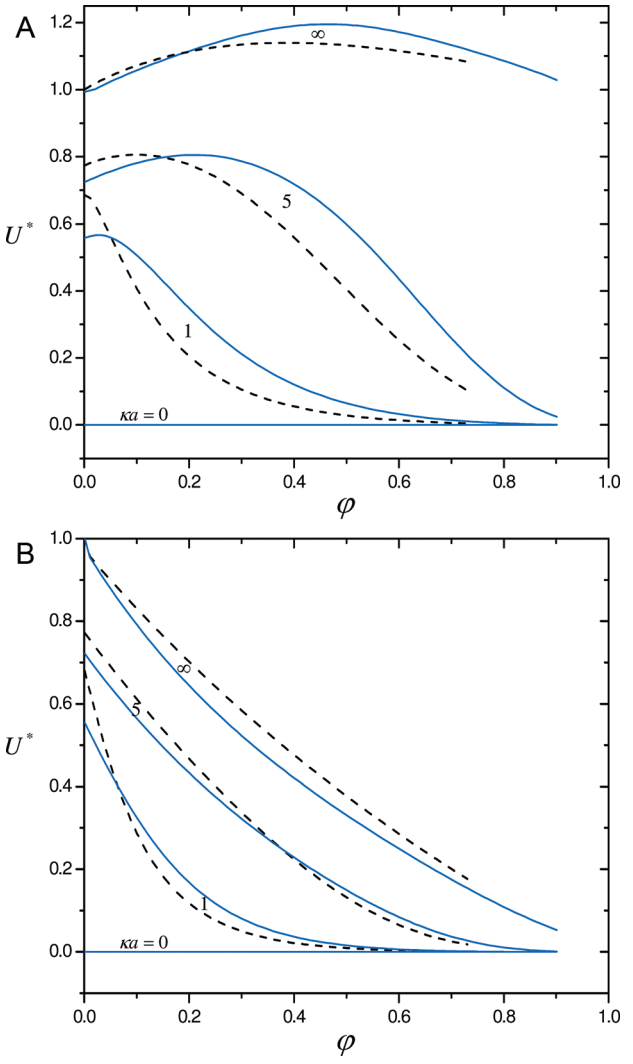

Figure 3. Plots of the normalized electroosmotic velocity U^* of an electrolyte solution through a transversely oriented fiber matrix versus φ with κa as a parameter: (a) the Happel/Levine−Neale cell model; (b) the Kuwabara/Zharkikh−Shilov cell model. The dashed curves are the corresponding results for a bed of spheres for comparison.

When the Levine−Neale electrokinetic cell model is used, the normalized electroosmotic velocity U^* is a monotonic decreasing function of φ for any given finite value of κa (and equals zero and unity as $\kappa a = 0$ and $\kappa a \rightarrow \infty$, respectively, regardless of the value of φ) for the case of the Kuwabara hydrodynamic cell model. However, for the case of the Happel hydrodynamic model, U^* is not a monotonic function of φ and has a maximum (whose value can be greater than unity) for a given finite value of κa. The location of this maximum shifts to greater φ as κa increases. On the other hand, when the Zharkikh−Shilov electrokinetic model is used, both the Happel and the Kuwabara hydrodynamic models predict that U^* decreases monotonically with an increase in φ for an arbitrary fixed value of κa. For any combination of κa and φ, the Kuwabara model results in a lower value of U^* (or a stronger porosity dependence for the electroosmotic velocity) than the Happel model does, which occurs because the zero-vorticity boundary condition yields a larger energy dissipation in the cell than that due to the drag on the cylinder alone, and the value of U^* predicted by the Zharkikh−Shilov model is always smaller than that predicted by the Levine−Neale model.

The corresponding results of the normalized electroosmotic velocity U^* for a bed of identical spheres[30] of radius a are also drawn by dashed curves in Figure 3 for comparison. These results are shown up to the maximum attainable volume fraction for a swarm of identical spheres, $\varphi = 0.74$.[19] For each cell model, the dependence of U^* on the parameters κa and φ for a bed of spheres is similar to that for an array of parallel cylinders. For a combination of κa and φ, the value of U^* is greater in a bed of spheres than in a fiber bed if the value of φ is low, and can be smaller in a bed of spheres than in a fiber bed if the value of φ is high. Existing experimental data on the electrophoretic mobility in suspensions of spherical particles[47−50] and rodlike particles[51,52] as functions of the volume fraction of the particles at low volume fractions in general indicate first an increase of the particle mobility, then a plateau, and finally a decrease. Our predictions of the Happel/Levine−Neale model in Figures 2a and 3a are compatible with this experimental outcome.

dx.doi.org/10.1021/jp203890n |J. Phys. Chem. B 2011, 115, 9168–9178

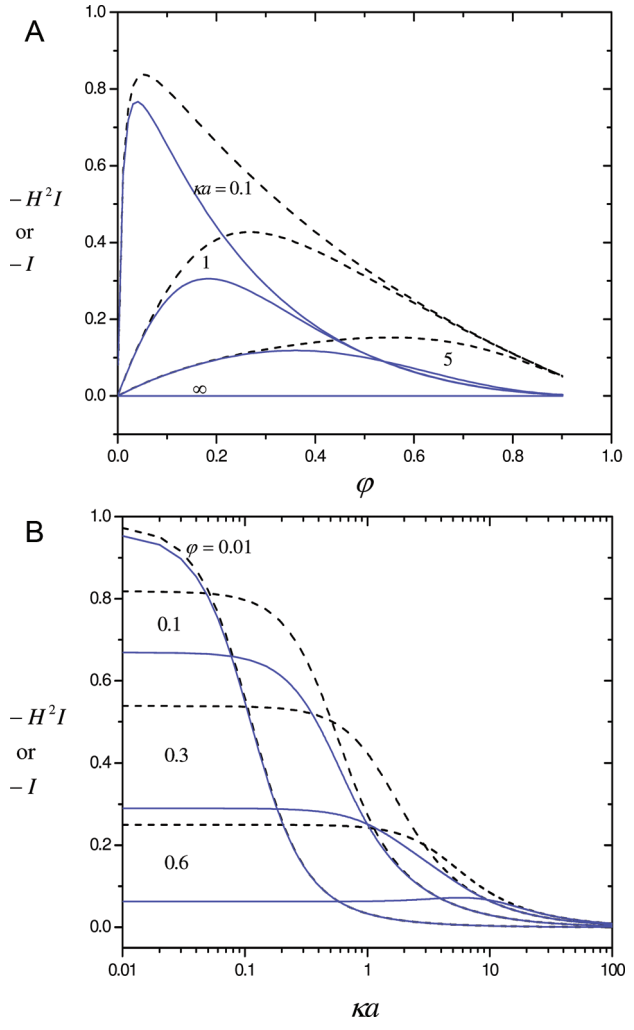

Figure 4. Plots of the dimensionless coefficients H^2I in eq 29a for the Levine−Neale cell model (solid curves) and I in eq 29b for the Zharkikh−Shilov cell model (dashed curves) for the effective conductivity in a transversely oriented fiber matrix versus the parameters κa and φ.

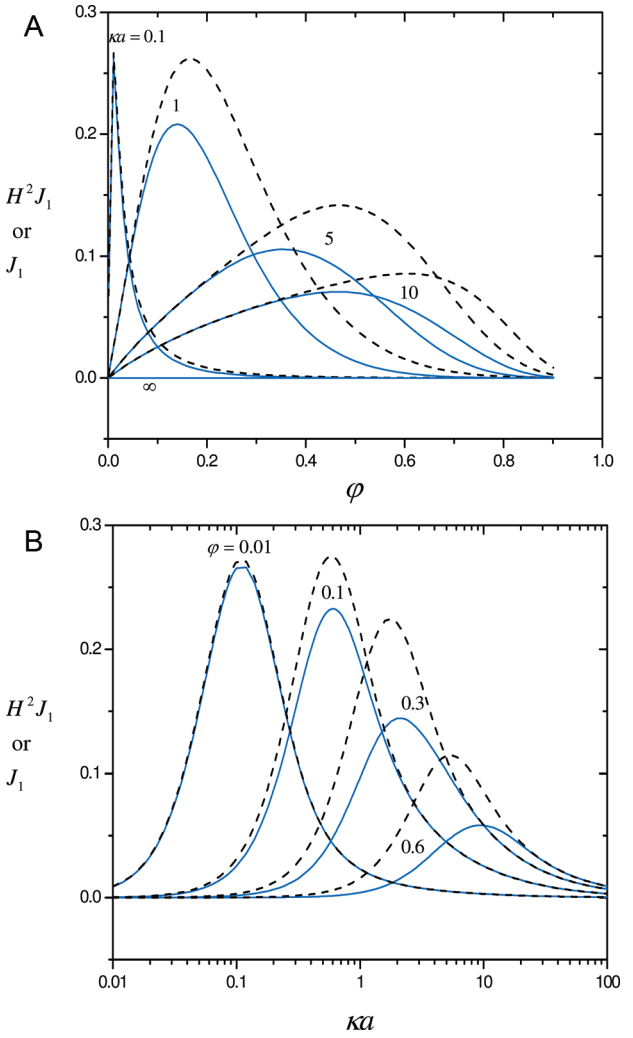

Figure 5. Plots of the dimensionless coefficients H^2J_1 in eq 29a for the Levine−Neale cell model (solid curves) and J_1 in eq 29b for the Zharkikh−Shilov cell model (dashed curves) for the effective conductivity in a transversely oriented fiber matrix versus the parameters κa and φ when the Happel hydrodynamic cell model is used.

5.2. Effective Electric Conductivity. In Figure 4, the dimensionless coefficients H^2I in eq 29a for the Levine−Neale model and I in eq 29b for the Zharkikh−Shilov model of the $O(\zeta)$ term for the effective electric conductivity in a transversely oriented fiber matrix are plotted for various values of the parameters κa and φ. Similar to the case of a bed of charged spheres,[30] these coefficients are always negative; thus, the presence of the surface charges on the cylinders increases the magnitude of the electric conductivity for any porosity of the fibrous medium if the product of β and ζ is negative and decreases this magnitude if $\beta\zeta > 0$. For a fixed value of κa, the effect of the surface charges on the electric conductivity is maximal at some value of φ and vanishes as $\varphi = 0$. The location of the maximum in $-I$ or $-H^2I$ shifts to greater φ as κa increases. For a fixed value of φ, $-I$ and $-H^2I$ in general are decreasing functions of κa and approach zero as $\kappa a \rightarrow \infty$. Different from the case of a bed of charged spheres, the value of $-I$ for the Zharkikh−Shilov model is always greater than that of $-H^2I$ for the Levine−Neale model for a specified combination of κa and φ; the difference between these two coefficients becomes smaller as the value of φ gets smaller or the value of κa gets greater.

Figure 5 shows the plots of the dimensionless coefficients H^2J_1 in eq 29a for the Levine−Neale model and J_1 in eq 29b for the Zharkikh−Shilov model of the $O(\zeta^2)$ term for the effective conductivity for various values of the parameters κa and φ. Unlike the coefficients H^2I and I presented in Figure 4, the values of H^2J_1 and J_1, which are positive, depend on the condition for the fluid velocity at the outer boundary of the unit cell. The values of H^2J_1 and J_1 predicted by the Happel model are larger than those predicted by the Kuwabara model, but in general, the difference is small. For a constant value of κa, the coefficients H^2J_1 and J_1 are not monotonic functions of φ and have maximal values. The locations of these maxima shift to greater φ as κa increases. For a given value of φ, maxima of the coefficients H^2J_1 and J_1 appear. As φ increases, these maxima occur at larger κa. In the limit of $\varphi = 0$, $\kappa a = 0$, or $\kappa a \rightarrow \infty$, H^2J_1 and J_1 vanish. Different from the case of a bed of charged spheres again, the value of J_1 for the Zharkikh−Shilov model is always greater than that of H^2J_1 for the Levine−Neale model for a given combination of κa and φ.

The dimensionless coefficients H^2J_2 in eq 29a for the Levine−Neale model and J_2 in eq 29b for the Zharkikh−Shilov model of

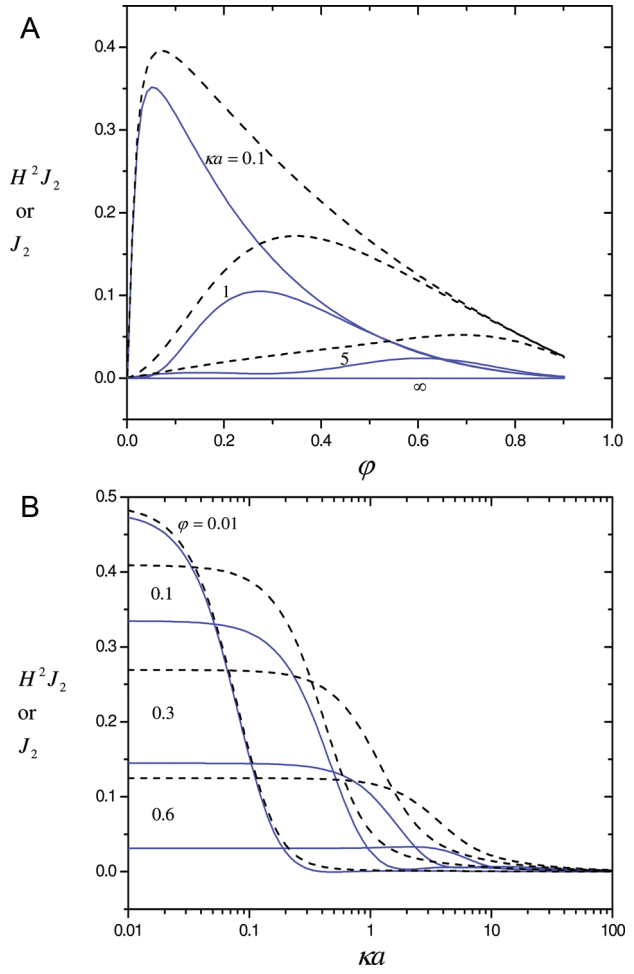

Figure 6. Plots of the dimensionless coefficients H^2J_2 in eq 29a for the Levine−Neale cell model (solid curves) and J_2 in eq 29b for the Zharkikh−Shilov cell model (dashed curves) for the effective conductivity in a transversely oriented fiber matrix versus the parameters κa and φ.

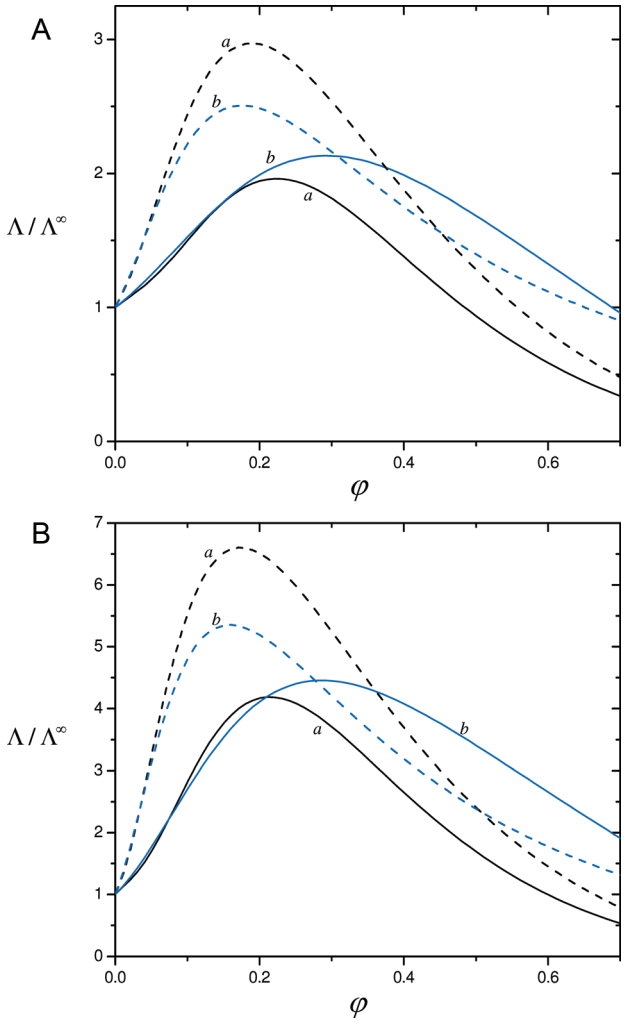

Figure 7. Plots of the normalized electric conductivity Λ/Λ^∞ for the aqueous solution of 0.1 mM $HClO_4$ in a transversely oriented fiber matrix (solid curves) and in a suspension of spheres (dashed curves) versus the parameter φ: (a) $\kappa a = 1.13$ and $\zeta = -62.2$ mV; (b) $\kappa a = 0.91$ and $\zeta = -99$ mV. Curves a and b are plotted for the Happel/Levine−Neale and Happel/Zharkikh−Shilov cell models, respectively.

the $O(\zeta^2)$ term for the effective conductivity are plotted in Figure 6 as functions of the parameters κa and φ. In general, the trend of the dependence for H^2J_2 and J_2 on κa and φ is analogous to that for H^2I and I, but the magnitudes of H^2J_2 and J_2 are smaller by a factor of about 2. For a constant value of φ, J_2 for the Zharkikh−Shilov model is a monotonic decreasing function of κa, but H^2J_2 for the Levine−Neale model is not; both coefficients approach zero as $\kappa a \rightarrow \infty$.

Watillon and Stone-Masui[42] measured the effective electric conductivities of suspensions of polystyrene latex spheres in 0.1 mM $HClO_4$ aqueous solutions at low particle volume fractions. Their experimental data for the cases of 70-nm-diameter spheres with a zeta potential of −62.2 mV (κa = 1.13) and 56-nm-diameter spheres with a zeta potential of −99 mV (κa = 0.91) have been compared with the predictions from the Happel spherical cell model.[30] In Figure 7, the normalized electric conductivity Λ/Λ^∞ for a homogeneous array of transversely oriented cylinders as calculated from eqs 29 for these cases is plotted versus the volume fraction φ of the cylinders in solid curves. Since the Happel and Kuwabara models give equivalent values of Λ/Λ^∞, only the results for the Happel model are presented. The corresponding cell-model results of Λ/Λ^∞ for a suspension of spheres are also drawn by dashed curves in the same figure for comparison. All these results indicate that the effective electric conductivity first increases with an increase in the volume fraction of the solid entities, reaches a maximum, and then decreases with a further increase in φ. This tendency agrees with recent experimental data[49] on the conductivity of a suspension of charged spherical particles at low volume fractions. For a fixed porosity, the Levine−Neale cell model predicts that the effective conductivity in an array of transversely oriented cylinders is smaller than that of a suspension of spheres. However, the Zharkikh−Shilov cell model predicts that the effective conductivity in an array of transversely oriented cylinders is smaller than that of a suspension of spheres when the value of φ is relatively small, and can be greater than that when φ becomes relatively high. The electric conductivity predicted by the Zharkikh−Shilov model can be either greater or smaller than that predicted by the Levine−Neale model, depending on the volume fraction φ. Note that the porosity effect (the effect of interactions among the cylinders or spheres) on the effective conductivity can be very significant under appropriate conditions.

dx.doi.org/10.1021/jp203890n |J. Phys. Chem. B 2011, 115, 9168–9178

6. CONCLUDING REMARKS

The transverse electroosmosis and electric conduction in a fibrous porous medium composed of a homogeneous array of parallel, identical, charged cylinders with an arbitrary thickness of the electric double layers and filled with an electrolyte solution is analyzed in this article using unit cell models with various boundary conditions at the outer surface of the cell. Solving the linearized electrokinetic equations applicable to the system of a cylinder in a unit cell by a regular perturbation method, we have determined the electroosmotic velocity of the electrolyte solution correct to the first order of the zeta potential ζ in eq 22 and the effective electric conductivity as a power series in ζ up to $O(\zeta^2)$ in eqs 29. Comparisons of the results of the electroosmotic velocity and electric conductivity among the unit cell models with different conditions for the electric potential and fluid velocity at the outer boundary of the cell have been made. In typical situations, the effect of interactions among the cylinders on the electroosmosis and electric conduction can be significant.

The unit cell models with various boundary conditions at the outer surface of the cell lead to somewhat different results of the electroosmotic velocity and electric conductivity. Although these results provide meaningful information for the porosity effects on the electroosmosis and electric conduction in fibrous media, we still need to assess which boundary conditions are most likely applicable. An earlier analysis of electrophoresis in suspensions of dielectric spheres with thin but polarized electric double layers[26] using the unit cell models with the same boundary conditions at the outer surface as the present work indicates that the tendency of the dependence of the normalized electrophoretic velocity on the particle volume fraction for the case of the electrokinetic boundary condition given by eq 7d (the Levine−Neale model) is not correct, in comparison with the ensemble-averaged result obtained by using the concept of statistical mechanics for dilute suspensions of dielectric spheres with thin but polarized double layers. The consequence that this boundary condition is not as accurate as the boundary condition in eq 8 (the Zharkikh−Shilov model) is probably due to the fact that the angular component of the electrochemical/electrostatic potential gradients at the outer surface of the cell is not specified in eq 7d. On the other hand, the predictions from the Levine−Neale model are unable to match some experimental data of the electrophoretic mobility and electric conductivity in suspensions of charged spherical particles, whereas the predictions from the Zharkikh−Shilov model are in full agreement with those experimental results.[25,53] Therefore, it is recommended that the results calculated from the Kuwabara hydrodynamic model described by eqs 7a and 7c with the electrokinetic boundary condition in eq 8 should be chosen for systems with thin double layers (large values of κa) because the zero-vorticity boundary condition 7c is consistent with the irrotational flow field generated by an electrophoretic particle with a thin double layer. For systems with moderate to thick double layers, however, the results obtained from the Happel model specified by eqs 7a and 7b with the boundary condition in eq 8 should be chosen since the free-surface boundary condition 7b has the advantage of not requiring an exchange of mechanical energy between the cell and the environment. Generally speaking, the predictions from the Happel and Kuwabara cell models are in numerical agreement to within 20% and result in the same behavior qualitatively. Although experimental results on the electrophoretic/electroosmotic velocity and electric conductivity are available in the literature for suspensions of charged spheres,[42,43,47−50] the relevant experimental data for fibrous systems would be needed to confirm the validity of our cell-model results at various ranges of κa and φ.

We set the net force exerted on the unit cell or the charged cylinder equal to zero in Section 3. Actually, this would give a velocity of the cylindrical fiber in the cell, and the fluid velocity is the negative of it. To hold a charged fiber fixed under an external electric field requires that a force be applied to the fiber, and the fluid will flow by it. This applied force would be equal in magnitude to the sum of the electric and hydrodynamic forces acting on the fiber translating transversely with the obtained electrophoretic/electroosmotic velocity. For the case of a dielectric sphere in a cell filled with an electrolyte solution, the analytical relation between the applied force and the translational velocity of the particle was derived.[15] Following the same procedure, one may calculate the applied force required to hold the charged cylinder fixed in a cell under an external electric field.

Throughout the analysis in this work, the assumption of small Dukhin number has been employed. Thus, the effect of excess surface conduction within the electric double layer on electrophoresis/electroosmosis[54,55] is not addressed. Also, for the case of porous media or suspensions at high particle volume fractions or low salt concentrations, the added counterions released from the particles when they get charged in solution and the additional ionic species originated from the contribution of dissociating molecularly dissolved carbon dioxide should not be negligible in any experiment. There has been some recent discussion about this point.[56]

For a general case of electroosmosis and electric conduction in a fibrous system constructed by an array of parallel cylinders on an arbitrary angle relative to the cylinder axes, the imposed electric field can be taken as a combination of its transversal and longitudinal components with respect to the orientation of the cylinders. Hence, the general problem can be divided into two, if it is linearized as done in Section 2, and they might be separately solved. The overall electroosmotic velocity and electric conductivity of the bulk fluid can be obtained by the vectorial/tensorial combination of the two-component results. Since the problem of the transverse electroosmosis and electric conduction in a homogeneous array of parallel cylinders has been solved in the present paper, in a future work one only needs to treat the electroosmosis and electric conduction in the array generated by a longitudinal electric field.

APPENDIX: DEFINITIONS OF SOME FUNCTIONS IN SECTION 3

The functions $F_{1\rho}(\rho)$, $F_{1\varphi}(\rho)$, $F_{p1}(\rho)$, and $F_{m1}(\rho)$ in eqs 19 and 20 are listed here:

$$F_{1\rho}(\rho) = C_1 + C_2 \ln\frac{\rho}{a} + C_3\left(\frac{a}{\rho}\right)^2 + C_4\left(\frac{\rho}{a}\right)^2 + \left[(\ln\rho)\int_a^\rho \left(\frac{\rho}{a}\right)^2 G(\rho)\mathrm{d}\rho - \int_a^\rho \left(\frac{\rho}{a}\right)^2 (\ln\rho)G(\rho)\mathrm{d}\rho - \frac{1}{4}\left(\frac{\rho}{a}\right)^2\int_a^\rho G(\rho)\mathrm{d}\rho + \frac{1}{4}\left(\frac{a}{\rho}\right)^2\int_a^\rho \left(\frac{\rho}{a}\right)^4 G(\rho)\mathrm{d}\rho\right] \quad \text{(A1a)}$$

$$F_{1\phi}(\rho) = -F_{1\rho}(\rho) - \rho\frac{\mathrm{d}F_{1\rho}}{\mathrm{d}\rho} \quad \text{(A1b)}$$

$$F_{p1}(\rho) = -2C_2\frac{a}{\rho} + 8C_4\frac{\rho}{a} - 2\left[\frac{\rho}{a}\int_a^\rho G(\rho)\mathrm{d}\rho + \frac{a}{\rho}\int_a^\rho \left(\frac{\rho}{a}\right)^2 G(\rho)\mathrm{d}\rho\right] \quad \text{(A1c)}$$

$$F_{m1}(\rho) = \frac{z_m^2 e^2 \rho}{2kT\chi}\left\{\frac{1}{\chi}[A_{\mu 1}(a,b) + (1-\chi)B_{\mu 1}(a,b)]\left[1+\left(\frac{a}{\rho}\right)^2\right] - A_{\mu 1}(a,\rho) + \left(\frac{a}{\rho}\right)^2 B_{\mu 1}(a,\rho)\right\} \quad (A2)$$

where

$$G(\rho) = -\frac{\varepsilon\kappa^2 a^2}{4\eta\chi}\left[1+\left(\frac{a}{\rho}\right)^2\right]\frac{d\psi_{eq1}}{d\rho} \quad (A3)$$

$$A_{\mu 1}(x,y) = \int_x^y \left[1-\left(\frac{a}{\rho}\right)^2\right]\frac{d\psi_{eq1}}{d\rho}\,d\rho \quad (A4a)$$

$$B_{\mu 1}(x,y) = \int_x^y \left[\left(\frac{\rho}{a}\right)^2 - 1\right]\frac{d\psi_{eq1}}{d\rho}\,d\rho \quad (A4b)$$

the function $\psi_{eq1}(\rho)$ was given by eq 10, and the coefficient χ was defined right after eq 14. The constants C_i with $i = 1, 2, 3$, and 4 in eqs A1 are

$$C_1 = [(-1+\varphi^2)A_1 + 2\varphi\ ln\ \varphi B_1]\omega \quad (A5a)$$

$$C_2 = [2(1+\varphi^2)A_1 + 4\varphi B_1]\omega \quad (A5b)$$

$$C_3 = [A_1 + (1-ln\ \varphi)\varphi B_1]\omega \quad (A5c)$$

$$C_4 = [-\varphi^2 A_1 - (1+ln\ \varphi)\varphi B_1]\omega \quad (A5d)$$

$$A_1 = \frac{U_1}{E_\infty} + \int_a^b \left(\frac{\rho}{a}\right)^2 ln\left(\frac{b}{\rho}\right)G(\rho)\,d\rho \quad (A6a)$$

$$B_1 = \frac{1}{4}\left(\frac{a}{b}\right)^2\int_a^b\left(\frac{\rho}{a}\right)^4 G(\rho)\,d\rho - \frac{1}{4}\left(\frac{b}{a}\right)^2\int_a^b G(\rho)\,d\rho \quad (A6b)$$

for the Happel model, and

$$C_1 = \frac{1}{6}[4(-1+\varphi)A_1' - (1+2\varphi\ ln\ \varphi - \varphi^2)B_1']\omega' \quad (A7a)$$

$$C_2 = \frac{1}{3}[4A_1' + (1-2\varphi+\varphi^2)B_1']\omega' \quad (A7b)$$

$$C_3 = \frac{1}{6}[2(2-\varphi)A_1' + (1-\varphi+\varphi\ ln\ \varphi)B_1']\omega' \quad (A7c)$$

$$C_4 = \frac{1}{6}[-2\varphi A_1' + (\varphi+\varphi\ ln\ \varphi - \varphi^2)B_1']\omega' \quad (A7d)$$

$$A_1' = \frac{U_1}{E_\infty} + \int_a^b \left(\frac{\rho}{a}\right)^2 ln\left(\frac{b}{\rho}\right)G(\rho)\,d\rho + \frac{1}{4}\left(\frac{a}{b}\right)^2\int_a^b\left(\frac{\rho}{a}\right)^4 G(\rho)\,d\rho - \frac{1}{4}\left(\frac{b}{a}\right)^2\int_a^b G(\rho)\,d\rho \quad (A8a)$$

$$B_1' = -\int_a^b\left(\frac{\rho}{a}\right)^2 G(\rho)\,d\rho + \left(\frac{b}{a}\right)^2\int_a^b G(\rho)\,d\rho \quad (A8b)$$

for the Kuwabara model, where

$$\omega = (1-\varphi^2 + ln\ \varphi + \varphi^2\ ln\ \varphi)^{-1} \quad (A9a)$$

$$\omega' = \left(1-\frac{4}{3}\varphi+\frac{1}{3}\varphi^2+\frac{2}{3}\ ln\ \varphi\right)^{-1} \quad (A9b)$$

Note that, for a symmetrically charged electrolyte, $F_{+1} = F_{-1}$.

The functions $F_{\pm 2}(\rho)$ in eq 24 are listed here:

$$F_{\pm 2}(\rho) = \mp\frac{Ze\rho}{2kT}\left\{\frac{1}{\chi}[A_{\pm 2}(a,b) + (1-\chi)B_{\pm 2}(a,b)]\left[1+\left(\frac{a}{\rho}\right)^2\right] - A_{\pm 2}(a,\rho) + \left(\frac{a}{\rho}\right)^2 B_{\pm 2}(a,\rho)\right\} \quad (A10)$$

where

$$A_{\pm 2}(x,y) = \int_x^y\left[\frac{dF_{\pm 1}}{d\rho} - \frac{kT}{D_\pm}F_{1\rho}(\rho)\right]\frac{d\psi_{eq1}}{d\rho}d\rho \quad (A11a)$$

$$B_{\pm 2}(x,y) = \int_x^y\left(\frac{\rho}{a}\right)^2\left[\frac{dF_{\pm 1}}{d\rho} - \frac{kT}{D_\pm}F_{1\rho}(\rho)\right]\frac{d\psi_{eq1}}{d\rho}d\rho \quad (A11b)$$

and the functions $F_{1\rho}(\rho)$ and $F_{\pm 1}(\rho)$ are given by eqs A1a and A2, respectively.

AUTHOR INFORMATION

Corresponding Author

*Telephone: 886-2-33663048. Fax: +886-2-2362-3040. E-mail: huan@ntu.edu.tw.

ACKNOWLEDGMENT

This work was partly supported by the National Science Council of the Republic of China.

REFERENCES

(1) Henry, D. C. *Proc. R. Soc. London, Ser. A* **1931**, *133*, 106.
(2) Booth, F. *Proc. R. Soc. London, Ser. A* **1950**, *203*, 514.
(3) Dukhin, S. S.; Derjaguin, B. V. In *Surface and Colloid Science*; Matijevic, E., Ed.; Wiley: New York, 1974; Vol. 7.
(4) Saville, D. A. *J. Colloid Interface Sci.* **1979**, *71*, 477.
(5) O'Brien, R. W. *J. Colloid Interface Sci.* **1981**, *81*, 234.
(6) Ohshima, H.; Healy, T. W.; White, L. R. *J. Chem. Soc., Faraday Trans. 2* **1983**, *79*, 1613.
(7) O'Brien, R. W. *J. Colloid Interface Sci.* **1983**, *92*, 204.
(8) O'Brien, R. W.; White, L. R. *J. Chem. Soc., Faraday Trans. 2* **1978**, *74*, 1607.
(9) O'Brien, R. W.; Ward, D. N. *J. Colloid Interface Sci.* **1988**, *121*, 402.
(10) Happel, J. *AIChE J.* **1958**, *4*, 197.
(11) Happel, J. *AIChE J.* **1959**, *5*, 174.
(12) Kuwabara, S. *J. Phys. Soc. Jpn.* **1959**, *14*, 527.
(13) Levine, S.; Neale, G.; Epstein, N. *J. Colloid Interface Sci.* **1976**, *57*, 424.
(14) Ohshima, H. *J. Colloid Interface Sci.* **1998**, *208*, 295.
(15) Keh, H. J.; Ding, J. M. *J. Colloid Interface Sci.* **2000**, *227*, 540.
(16) Carrique, F.; Arroyo, F. J.; Delgado, A. V. *Colloids Surf., A* **2001**, *195*, 157.

(17) Lee, E.; Chou, K. T.; Hsu, J. P. *J. Colloid Interface Sci.* **2006**, *295*, 279.
(18) Keh, H. J.; Chen, W. C. *J. Colloid Interface Sci.* **2006**, *296*, 710.
(19) Levine, S.; Neale, G. H. *J. Colloid Interface Sci.* **1974**, *47*, 520.
(20) Zharkikh, N. I.; Borkovskaya, Yu. B. *Colloid J. USSR (Engl. Transl.)* **1982**, *43*, 520.
(21) Zharkikh, N. I.; Shilov, V. N. *Colloid J. USSR (Engl. Transl.)* **1982**, *43*, 865.
(22) Kozak, M. W.; Davis, E. J. *J. Colloid Interface Sci.* **1986**, *112*, 403.
(23) Ohshima, H. *J. Colloid Interface Sci.* **1997**, *188*, 481.
(24) Ohshima, H. *J. Colloid Interface Sci.* **1999**, *210*, 397.
(25) Dukhin, A. S.; Shilov, V.; Borkovskaya, Yu. *Langmuir* **1999**, *15*, 3452.
(26) Wei, Y. K.; Keh, H. J. *Langmuir* **2001**, *17*, 1437.
(27) Carrique, F.; Ruiz-Reina, E.; Arroyo, F. J.; Jimenez, M. L.; Delgado, A. V. *Langmuir* **2008**, *24*, 2395.
(28) Kozak, M. W.; Davis, E. J. *J. Colloid Interface Sci.* **1989**, *127*, 497.
(29) Johnson, T. J.; Davis, E. J. *J. Colloid Interface Sci.* **1999**, *215*, 397.
(30) Ding, J. M.; Keh, H. J. *J. Colloid Interface Sci.* **2001**, *236*, 180.
(31) Carrique, F.; Arroyo, F. J.; Jimenez, M. L.; Delgado, A. V. *J. Phys. Chem. B* **2003**, *107*, 3199.
(32) Carrique, F.; Cuquejo, J.; Arroyo, F. J.; Jimenez, M. L.; Delgado, A. V. *Adv. Colloid Interface Sci.* **2005**, *118*, 43.
(33) Keh, H. J.; Liu, C. P. *J. Phys. Chem. C* **2010**, *114*, 22044.
(34) Ohshima, H. *J. Colloid Interface Sci.* **1999**, *212*, 443.
(35) Lee, E.; Chih, M. H.; Hsu, J. P. *Langmuir* **2001**, *17*, 1821.
(36) Hsu., W. T.; Keh, H. J. *Colloid Polym. Sci.* **2004**, *282*, 985.
(37) Cuquejo, J.; Jimenez, M. L.; Delgado, A. V.; Arroyo, F. J.; Carrique, F. *J. Phys. Chem. B* **2006**, *110*, 6179.
(38) Keh, H. J.; Wei, Y. K. *Langmuir* **2002**, *18*, 10475.
(39) Wei, Y. K.; Keh, H. J. *J. Colloid Interface Sci.* **2002**, *248*, 76.
(40) Hsu, J.-P.; Lou, J.; He, Y.-Y.; Lee, E. *J. Phys. Chem. B* **2007**, *111*, 2533.
(41) Lou, J.; Lee, E. *J. Phys. Chem. C* **2008**, *112*, 12455.
(42) Watillon, A.; Stone-Masui, J. *J. Electroanal. Chem.* **1972**, *37*, 143.
(43) Zukoski, C. F.; Saville, D. A. *J. Colloid Interface Sci.* **1987**, *115*, 422.
(44) Anderson, J. L. *Ann. N.Y. Acad. Sci.* **1986**, *469* (Biochem. Eng. 4), 166.
(45) Happel, J.; Brenner, H. *Low Reynolds Number Hydrodynamics*; Nijhoff: Dordrecht, The Netherlands, 1983.
(46) Berryman, J. G. *Phys. Rev. A* **1983**, *27*, 1053.
(47) Bellini, T.; Degiorgio, V.; Mantegazza, F.; Marsan, F. A.; Scarnecchia, C. *J. Chem. Phys.* **1995**, *103*, 8228.
(48) Palberg, T.; Medebach, M.; Garbow, N.; Evers, M.; Fontecha, A. B.; Reiber, H.; Bartsch, E. *J. Phys.: Condens. Matter* **2004**, *16*, S4039.
(49) Medebach, M.; Jordan, R. C.; Reiber, H.; Schope, H.-J.; Biehl, R.; Evers, M.; Hessinger, D.; Olah, J.; Palberg, T.; Schonberder, E.; Wette, P. *J. Chem. Phys.* **2005**, *123*, 104903.
(50) Lobaskin, V.; Dunweg, B.; Medebach, M.; Palberg, T.; Holm, C. *Phys. Rev. Lett.* **2007**, *98*, 176105.
(51) Deggelmann, M.; Graf, C.; Hagenbuchle, M.; Hoss, U.; Johner, C.; Kramer, H.; Martin, C.; Weber, R. *J. Phys. Chem.* **1994**, *98*, 364.
(52) Hoss, U.; Batzill, S.; Deggelmann, M.; Graf, C.; Hagenbuchle, M.; Johner, C.; Kramer, H.; Martin, C.; Overbeck, E.; Weber, R. *Macromolecules* **1994**, *27*, 3429.
(53) Cuquejo, J.; Jimenez, M. L.; Delgado, A. V.; Arroyo, F. J.; Carrique, F. *J. Phys. Chem. B* **2006**, *110*, 6179.
(54) Levin, Y. *Rep. Prog. Phys.* **2002**, *65*, 1577.
(55) Messinger, R. J.; Squires, T. M. *Phys. Rev. Lett.* **2010**, *105*, 144503.
(56) Carrique, F.; Ruiz-Reina, E. *J. Phys. Chem. B* **2009**, *113*, 8613.